Research Square

Preprints are preliminary reports that have not undergone peer review.
They should not be considered conclusive, used to inform clinical practice,
or referenced by the media as validated information.

A gibberellin-responsive MYB transcription factor controls internal browning in pineapple

Han He
Institute of Fruit Tree Research, Guangdong Academy of Agricultural Sciences
Chuanhe Liu
founderlch@126.com
Institute of Fruit Tree Research, Guangdong Academy of Agricultural Sciences
Min Yang
Institute of Fruit Tree Research, Guangdong Academy of Agricultural Sciences
Yuerong Wei
Institute of Fruit Tree Research, Guangdong Academy of Agricultural Sciences
Ruibin Kuang
Institute of Fruit Tree Research, Guangdong Academy of Agricultural Sciences
Chenping Zhou
Institute of Fruit Tree Research, Guangdong Academy of Agricultural Sciences
Xiaming Wu
Institute of Fruit Tree Research, Guangdong Academy of Agricultural Sciences
Yanzhao Sun
Institute of Fruit Tree Research, Guangdong Academy of Agricultural Sciences

Research Article

Keywords: Pineapple, AcMYB108, Internal browning, Gibberellin, Postharvest senescence

Posted Date: September 3rd, 2026

DOI: https://doi.org/10.21203/rs.3.rs-10607982/v1

License: This work is licensed under a Creative Commons Attribution 4.0 International License.
Read Full License

Additional Declarations: No competing interests reported.

Abstract

Background

Internal browning (IB) is a prevalent postharvest disorder in pineapple that causes substantial economic losses due to its delayed symptom manifestation. While the chilling-induced membrane dysfunction model has been the prevailing explanation for IB development, emerging evidence implicates fruit ripening stage and phytohormonal regulation as critical determinants, yet the underlying molecular mechanisms remain poorly understood.

Result

Through integrated transcriptomic, DAP-seq and biochemical analyses, we demonstrate that AcMYB108 directly activates two WRKY transcription factors, AcWRKY31 and AcWRKY75, which subsequently trigger the expression of the senescence-associated cysteine protease AcSAG12 to mediate cellular degradation and browning manifestation. Furthermore, we elucidate a dual regulatory mechanism by which gibberellin exacerbates IB severity through both transcriptional activation of *AcMYB108* and destabilization of the inhibitory AcWRKY75-AcDELLA interaction.

Conclusion

our findings characterize an AcMYB108 signaling cascade as a central hub integrating senescence and hormonal signals to regulate pineapple IB, establishing a mechanistic framework that explains how fruit maturity and GA treatment influence disorder susceptibility, and offering critical insights for optimizing preharvest GA application strategies to mitigate postharvest losses in pineapple.

Introduction

Pineapple (*Ananas comosus* L.) ranks as the third most important tropical fruit in international trade, with an annual market value exceeding 2.5 billion U.S. dollars[1]. However, maintaining the freshness of the postharvest pineapples is severely threatened by internal browning (IB), a disorder characterized by translucency and brown discoloration at the fruitlet base near the core[2]. Because IB lacks visible external symptoms, it is typically goes undetected until consumption, severely undermines consumer satisfaction and leading to substantial economic losses[3].

Multiple environmental and developmental factors influence IB development. Although low temperature storage is widely used to extend shelf life, prolonged cold storage induces chilling injury and promotes IB development[4–6]. Phytohormones also play critical roles: ethylene and gibberellin (GA) promote IB, while abscisic acid (ABA) alleviates it[3, 7]. Harvest maturity is another decisive factor, as over-ripe or late-harvested fruits exhibit significantly higher incidence of browning index[8, 9].

Although these factors have been extensively documented, the underlying mechanisms are not fully understood and have been reinterpreted over time. IB was initially proposed as a PPO-driven physiological disorder, with PPO activation regarded as the initiating event[10]. However, subsequent studies have reported poor or inconsistent correlations between measured PPO activity and the incidence of internal browning, suggesting that PPO alone does not determine IB development[11, 12]. In recent decades, extensive studies have established that IB primarily results from membrane damage induced by low temperature stress[5, 13]. Low temperature storage causes membrane damage through two distinct mechanisms. First, low temperatures alter the lipid composition of the plasma membrane, leading to phospholipid loss, reduced phosphatidylinositol levels and decreased fatty acid unsaturation, thereby disrupting the structural integrity of cell membranes[5]. Second, low temperatures also trigger the overproduction of reactive oxygen species (ROS), as evidenced by increased levels of H_2O_2 and lipoxygenases (LOXs) reported during IB development The excessive accumulation of ROS induces lipid peroxidation, further compromising membrane integrity and disrupting cellular compartmentalization. This decompartmentalization enables plastidic PPO to come into contact with its phenolic substrates in the vacuole. The resulting o-quinones are ultimately converted into colored polymers, which directly contribute to browning symptoms[6, 14].

Despite these extensive physiological and biochemical characterizations, the molecular mechanisms underlying IB development remain largely elusive. Moreover, the current chilling-induced membrane damage model still cannot adequately explain how other environmental and developmental factors beyond low temperature influence IB development. For instance, exogenous GA_3 has been proven to induce IB even under normal temperatures[15]. Additionally, IB is more severe in half-ripe fruits than in those at the color break stage[9].

To address these knowledge gaps, we conducted a comparative transcriptomic analysis of ‘Comte de Paris’ pineapples to identify key genes and pathways governing internal browning development. In this study, we identified and characterized a pineapple R2R3 MYB transcription factor, AcMYB108, that plays a regulatory role in IB development. We further demonstrate that upregulation of AcMYB108 promotes IB by directly activating two WRKY transcription factors, AcWRKY31 and AcWRKY75, which subsequently induce the expression of the senescence-associated cysteine protease AcSAG12. Moreover, we uncover a dual regulatory mechanism by which GA signaling exacerbates IB through both transcriptional activation of AcMYB108 and destabilization of the inhibitory AcWRKY75-AcDELLA interaction. Collectively, these findings establish an AcMYB108-mediated signaling cascade as a central regulator of pineapple internal browning, providing mechanistic insights into how fruit maturity and GA treatment influence IB development and offering a framework for optimizing preharvest management to reduce postharvest losses.

Materials and methods

Pineapple (*Ananas comosus* L. Merr.) fruits at the yellow-ripe maturity stage were purchased from Tianping Fruit Market in Tianhe District, Guangzhou, China. Fruits of uniform size and without visible defects were selected for experiments. All fruits were divided into two groups and subjected to either low temperature (10^{o}C) or room temperature (25^{o}C). Pulp sample tissues were collected every two days, immediately frozen in liquid nitrogen, and stored at -80^{o}C for further analyses.

For transient overexpression analysis, the experimental hemisphere of each pineapple fruit was injected at the equatorial line with *Agrobacterium tumefaciens* carrying the pGreenII-62-SK: *AcMYB108* (OE) vector, while the contralateral hemisphere was injected with *Agrobacterium tumefaciens* carrying the empty vector pGreenII-62-SK (EV). Three independent biological replications were performed, each containing five randomly selected fruits. After infiltration, all fruits were sealed with parafilm to maintain humidity and incubated at 25^{o}C under 70% relative humidity for 48 hours prior to analysis.

Transcriptomic analysis

Transcriptomic analysis was performed on pineapple pulp tissues at the onset of browning (6 days at 25°C): browning pulp (BP) and adjacent non-browning pulp (AP) from the IB-affected fruits, and healthy control pulp (CK) from fruits without IB symptoms. RNA-seq library construction and sequencing„ including total RNA isolation, mRNA enrichment, cDNA synthesis, library construction and paired-end sequencing was performed by BGI Genomics Co., Ltd. (Shenzhen, China).

Raw sequencing reads were filtered with Trimmomatic software to remove adapter reads and low quality sequences. Clean reads were aligned to the reference genome of *Ananas comosus* (ASM154086v1) using HISAT (v2.2.1) with default parameters, followed by transcript quantification via RSEM (v1.3.3) to generate FPKM (Fragments Per Kilobase of Transcript per Million Mapped Reads) values for expression analysis. Differential expression analysis was conducted with DESeq, using a threshold of $|\log_2$ fold change$| \geq 1$ and FDR ≤ 0.01. Genes were assigned to GO and KEGG enrichment analysis using Blast2GO. GO terms with a P value ≤ 0.05 were considered statistically significant, and the criteria for KEGG enrichment analysis were set at a P value ≤ 0.05 and a Q value ≤ 0.01.

Quantitative real-time PCR (qPCR) analysis

Total RNA was extracted using a plant RNA extraction kit (TIANDZ, China) following the manufacturer's protocol. cDNA synthesis was performed in 20 µL reactions containing 1 µg of total RNA using the PrimeScript™ RT Reagent Kit (Takara Bio, Japan). Quantitative real-time PCR (qPCR) was conducted on a QuantStudio™ 5 System (Applied Biosystems, USA) using TB Green® Premix Ex Taq (Takara Bio, Japan). Primers used in this study are listed in Table S1. Relative gene expression was calculated using the $2^{-\Delta\Delta Ct}$ method, with *β-actin* as the endogenous control.

DAP-Seq assays

DAP-seq assays were performed according to the method described by Bartlett et al. [16]. The Halo-AcMYB108 recombinant protein was expressed using the TNT SP6 Coupled Wheat Germ Extract System (Promega, USA) and purified with the Magne Halo-Tag beads (Promega, USA). Enriched genomic DNA (gDNA) was fragmented (~ 200 bp) using a Covaris M220 ultrasonicator (Woburn, USA). The resulting gDNA fragments were end repaired, A-tailed, and ligated to Illumina sequencing adapters. The gDNA library was incubated with the recombinant protein for 1h at 25°C. Captured DNA was amplified with TruSeq primers and sequenced on an Illumina HiSeq 4000 platform. Raw reads were processed to remove adapters and low quality reads, and the filtered reads were mapped to the reference genome of *Ananas comosus* (ASM154086v1) using Bowtie2 (v2.2.5). Peak calling was performed with MACS2 (v2.1.2) using HaloTag controls as background. Peak annotations were analyzed using the ChIPseeker R package, and de novo motif discovery was performed with MEME-chip (v5.4.1) with default parameters.

Yeast one-hybrid assay

Yeast one-hybrid assays were performed using the Matchmaker™ Gold Yeast One-Hybrid System (Clontech Laboratories, USA). The ORF of the AcMYB108 transcription factor was cloned into the pGADT7 vector to construct the pGADT7-AcMYB108 vector. The promoter regions of *AcWRKY31* and *AcWRKY75* were cloned into the pAbAi vector and subsequently integrated into the genome of the Y1HGold yeast strain, respectively. The pGADT7-AcMYB108 vector was then transformed into the Y1HGold (*AcWRKY31*) and Y1HGold (*AcWRKY75*) strains, with pGADT7 serving as a negative control. Protein-DNA interactions were confirmed by serial dilution on SD/Leu/Ura/AbA plates after incubation at 30°C for 3–5 days.

Yeast two-hybrid assay

The Matchmaker™ Gold Yeast Two-Hybrid System (Clontech Laboratories, USA), which contains four reporter genes (*AUR1-C*, *HIS3*, *ADE2* and *MEL1*), was used to detect protein-protein interactions. The ORFs of *AcWRKY75* and *AcDELLA* were cloned into the pGBKT7 and pGADT7 vectors, respectively, to generate recombinant plasmids. The resulting pGBKT7-AcWRKY75 and pGADT7-AcDELLA were co-transformed into the Y2HGold yeast strain to generate reporter strains, with pGBKT7 empty vector plus pGADT7-AcDELLA and pGBKT7-AcWRKY75 plus pGADT7 empty vector serving as negative controls.

EMSA

EMSA was performed using the Lightshift Chemiluminescent EMSA kit (Thermo Fisher Scientific, USA) according to the manufacturer's instructions. The ORF of *AcMYB108* was cloned into the pET-28a(+) vector to generate the recombinant plasmid pET-28a-AcMYB108. The plasmid was then transformed into *Escherichia coli* BL21(DE3), induced with 0.5 mM IPTG, and the His-tagged recombinant protein was

purified under native conditions using an His-Tagged Protein Purification Kit (ComWin Biotech, Beijing, China).

For binding reactions, biotin-labeled DNA probes containing 20 bp target sequences from the promoters of *AcW*RKY31 or AcWRKY75 were incubated with the purified AcMYB108 protein in binding buffer (50 ng/μL poly(dI·dC), 2.5% glycerol, 5 mM $MgCl_2$ and 0.05% NP-40) in the dark at 25°C for 30 min. The protein-DNA complexes were separated on a pre-run 6% native polyacrylamide gel in 0.5× TBE buffer at 300 V. Following electrophoresis, the separated complexes were transferred to a positively charged nylon membrane via semi-dry electroblotting and crosslinked by UV irradiation. Biotin-labeled DNA was detected using the Chemiluminescent Nucleic Acid Detection Module (Thermo Fisher Scientific, USA) according to the manufacturer's protocol, and signals were visualized using a ChemiDoc MP Imaging System (Bio-Rad). For competition assays, mutant probes were included as specificity controls.

Subcellular localization

The ORF of *AcMYB108* (excluding the stop codon) was cloned into the pAN580-GFP vector, placing the GFP gene downstream of the CaMV 35S promoter. The recombinant pAN580-AcMYB108-GFP plasmid and the nuclear marker NLS-mCherry were co-transfected into pineapple leaf protoplasts prepared according to a previously described method[17]. After incubation at 22°C in the dark for 16h, GFP and mCherry fluorescence signals were captured using a Leica confocal laser scanning microscope.

BiFC assay

The ORFs of *AcWRKY75* and *AcDELLA*, excluding stop codons, were individually cloned into the split-YFP vectors pSAT6-nEYFP-C1 and pSAT6-cEYFP-C1 to generate N-terminal and C-terminal YFP fusion constructs, respectively. For BiFC analysis, pineapple leaf protoplasts were co-transformed with pairwise combinations of the fusion constructs (AcWRKY75-YFPn with AcDELLA-YFPc and AcWRKY75-YFPc with AcDELLA-YFPn) using a PEG-mediated transient transformation[18]. As negative controls, empty YFPn and YFPc vectors were co-transformed with each fusion construct. After incubation at 25°C for 16–20 h, YFP signals were visualized using a confocal laser scanning microscope (Leica, Germany) with excitation at 488 nm and emission detection at 520–540 nm.

Dual luciferase transient expression assay

The coding sequence of *AcMYB108* was cloned into the pGreenII-62-SK vector to generate the effector construct pGreenII-62-SK-MYB108 (35S::AcMYB108). The promoter regions of *AcWRKY31* and *AcWRKY75* were cloned into the pGreenII-0800-LUC reporter vector, generating the reporter constructs pAcWRKY31::LUC and pAcWRKY75::LUC, respectively. All recombinant plasmids were introduced into *Agrobacterium tumefaciens* strain GV3101 via freeze-thaw transformation.

For co-infiltration, bacterial cultures (OD_{600}=0.8) harboring the effector and reporter constructs were mixed at a 1:1 ratio. As a negative control, bacterial cultures harboring the empty pGreenII-62-SK vector

were mixed with the reporter construct at the same ratio. The mixed suspensions were infiltrated into fully expanded leaves of 4-week-old *Nicotiana benthamiana* plants grown under controlled conditions (22°C, 16 h light/8 h dark, 60% humidity). Dual luciferase assays were performed 48h post-infiltration as described by Niu et al[19]. Firefly luciferase (LUC) activity was normalized to Renilla luciferase (REN) using the Dual-Luciferase® Reporter Assay System (Promega). Chemiluminescence images were captured using a Tanon-5200 Live Plant Imaging System (Tanon, China) with 5 min exposures. Three independent biological replicates were analyzed, each containing at least 6 infiltrated leaves.

Results

Internal browning in pineapple correlates with activation of senescence-associated pathways and upregulation of *AcMYB108*

To elucidate the molecular mechanisms underlying IB, we performed a comparative transcriptome analysis on three pulp tissue types at the onset of browning (day 6 at 25°C): browning pulp (BP) and adjacent non-browning pulp (AP) from the same IB fruit, and control pulp (CK) from healthy fruit. Compared with CK, BP exhibited 3,360 up-regulated and 5,422 down-regulated genes and AP showed 1,897 up-regulated and 2,066 down-regulated genes ($|\log_2 FC| \geq 1$, FDR ≤ 0.01). Across both comparisons, 1,624 up-regulated and 1,713 down-regulated genes were consistently differentially expressed, defining a core gene set potentially relevant to IB development (Fig. 1).

GO enrichment analysis of the 1,624 consistently up-regulated DEGs revealed significant enrichment in senescence-associated processes, including membrane integrity, stress response, phytohormone signaling, and programmed cell death. By contrast, down-regulated DEGs were predominantly associated with photosynthesis (Fig. 2). KEGG pathway analysis further showed that up-regulated DEGs were enriched in α-linolenic acid metabolism (ko00592) and N-glycan biosynthesis (ko00510), both linked to senescence and programmed cell death, while down-regulated DEGs were enriched in photosystem I and II components (Fig. 3). Collectively, these results establish a strong functional link between IB and accelerated senescence, providing a mechanistic basis for the observed influence of fruit maturity on IB susceptibility.

Among the up-regulated DEGs, we identified AcMYB108 (LOC109718059), an R2R3-MYB transcription factor showing 9.34- and 11.52-fold increases in AP and BP, suggesting its involvement in IB. qRT-PCR analysis of time-course samples revealed that its transcript levels at 25°C peaked at day 6, coinciding with symptom emergence; whereas at 10°C no such peak was observed and no browning developed (Fig. 4A).

AcMYB108 is a nucleus-localized transcriptional activator

To characterize the function of AcMYB108, we first examined its subcellular localization. AcMYB108-GFP fusion protein expressed in pineapple protoplasts exhibited exclusive nuclear localization, colocalizing with the nuclear marker NLS-mCherry (Fig. 4C). We next assessed its transcriptional

activation activity using a yeast transactivation system. Both full-length AcMYB108 and its C-terminal truncation variant activated reporter gene expression, confirming that AcMYB108 functions as a transcriptional activator with its activation domain located at the C-terminus (Fig.4D). An in-depth analysis of tissue-specific transcriptome data retrieved from the SRA database (SRP156886) revealed that revealed that AcMYB108 was predominantly expressed in reproductive organs, with minimal transcript accumulation in roots and leaves (Fig. 4E), suggesting a potential role in regulating postharvest internal browning.

To verify its role in internal browning, we performed *Agrobacterium*-mediated transient overexpression in pineapple fruit. Tissues infiltrated with the pGreenII-62-SK-AcMYB108 construct (OE) exhibited significantly enhanced browning around the inoculation sites compared with empty vector (EV) controls (Fig.4B). Collectively, these findings indicate that AcMYB108 is a nucleus-localized transcriptional activator whose upregulation promotes senescence-associated internal browning in postharvest pineapple fruit.

AcMYB108 regulates internal browning by targeting the promoters of *AcWRKY31* and *AcWRKY75*

To identify downstream target genes of AcMYB108, we performed DAP-seq analysis. A total of 7,011 genomic binding peaks were identified, with an average length of 536 bp, covering 1.19% of the pineapple genome (Fig. 5A). *De novo* motif discovery uncovered a conserved 7-bp binding motif (ACC[A/T]AA[T/C]), matching the AtMYB108 binding motif (MA2026) in the JASPAR database (Fig. 5B). Integration of DAP-seq with RNA-seq data identified 790 DEGs harboring this motif within their promoter regions, including two senescence-associated WRKY transcription factors, *AcWRKY31* and *AcWRKY75*.

To test whether AcMYB108 directly binds to these two WRKY promoters, Y1H and EMSA assays were performed. In the Y1H assays, the promoters of *AcWRKY31* and *AcWRKY75* were individually cloned into the pAbAi vector and integrated into the Y1HGold yeast genome (Fig. 6A). The resulting reporter strains transformed with pGADT7-AcMYB108 could grow on SD/-Leu/AbA medium, indicating that AcMYB108 binds to both promoters in vivo (Fig. 6B). Promoter sequence analysis identified the putative MYB-binding motifs, TTTACCAAACTTTTA and TGTACCTAACATTTT, within the upstream regions of *AcWRKY31* and *AcWRKY7*, respectively. EMSA confirmed that these motifs were specifically bound by the purified AcMYB108 protein (Fig. 6C). Dual-luciferase assays further confirmed that AcMYB108 transcriptionally activates the AcWRKY31 and AcWRKY75 promoters, as co-expression with the respective reporter constructs increased the LUC/REN ratio by 1.57-fold and 3.98-fold, respectively, compared with the empty vector control (Fig. 7).

We next examined whether these WRKYs regulate downstream senescence-associated effector genes. Y1H assays showed that AcWRKY75 directly bound to the promoter of AcSAG12, which encodes a cysteine protease serving as a senescence biomarker (Fig. S1A). qRT-PCR analysis showed that *AcWRKY75* and AcSAG12 displayed similar expression patterns as *AcMYB108* during storage: at 25°C, their transcript levels peaked at the onset of browning, whereas at 10 °C no such peak was observed and no browning symptoms developed (Fig. S1B). Together, these results identify a regulatory cascade in

which AcMYB108 activates AcWRKY75, which in turn promotes AcSAG12 expression to mediate IB progression.

GA promotes internal browning through the AcMYB108 cascade

Given that exogenous GA exacerbates internal browning in postharvest pineapple, we examined whether this phytohormone acts through the AcMYB108 regulatory pathway. Cis-element analysis of the AcMYB108 promoter revealed multiple conserved GA-responsive elements, including GARE and P-box motifs (Fig. S2A), suggesting direct transcriptional regulation by GA. GA treatment induced *AcMYB108* transcription in pineapple protoplasts, with transcript levels reaching a peak of approximately 5-fold at 12 h post-treatment (Fig. S2B).

In *Arabidopsis*, DELLA proteins, key repressors of GA signaling, suppress WRKY75 transcriptional activity through direct interaction. To test whether this regulatory module is conserved in pineapple, we performed a yeast two-hybrid screening using pGBKT7-AcWRKY75 as bait against a pineapple cDNA library under high-stringency conditions. This screen identified AcDELLA (LOC109713571) as a direct interactor of AcWRKY75. Reciprocal yeast two-hybrid assays confirmed the interaction, as yeast co-expressing BD-AcWRKY75 and AD-AcDELLA grew and turned blue on selective medium (QDO/X-α-gal) (Fig. 8A). Bimolecular fluorescence complementation (BiFC) assays in pineapple protoplasts further validated this interaction in planta: nuclear YFP fluorescence was detected in both reciprocal fusion combinations, but not in the negative controls (Fig. 8B).

Discussion

Internal browning (IB) in pineapple has long been interpreted through a chilling-induced membrane damage model, in which low temperature compromises membrane integrity and enables polyphenol oxidase to access phenolic substrates[5,6]. Yet this framework has struggled to accommodate persistent inconsistencies: exogenous GA promotes IB even under non-chilling conditions[20,21], fruit maturity at harvest markedly influences disorder susceptibility[9], and atmospheric stresses including hypercapnic or hypoxic conditions can similarly trigger physiological deterioration[22]. These observations cannot be simply explained by cold-induced membrane damage alone, pointing to the involvement of additional regulatory mechanisms.

Our transcriptomic results indicate that IB fruits exhibit pronounced enrichment of senescence-related pathways, including programmed cell death, membrane lipid degradation, and stress signaling, rather than merely genes associated with redox imbalance and membrane damage. This senescence-related transcriptional reprogramming was functionally validated by ethylene treatment. Given that ethylene is a well-documented inducer of plant senescence[23], and that exogenous ethylene application significantly enhanced IB incidence whereas the ethylene inhibitor 1-methylcyclopropene (1-MCP) effectively suppressed it, these results collectively confirm the intrinsic link between IB and senescence programs[24]. Interestingly, the inhibitory effect of 1-MCP is not restricted to pineapple IB[25, 26]; it also

alleviates a range of IB-like postharvest disorders, including kiwifruit watersoaking[27], avocado internal browning[28], apple and pear core browning[29, 30], and okra browning[31].

MYB transcription factors constitute one of the largest plant transcription factor families and play critical roles in regulating diverse developmental processes including senescence[32]. In *Arabidopsis*, AtMYB108 accelerates leaf senescence by directly activating *ANAC003*[33], while RhMYB108 in Rosa hybrida promotes petal senescence via targeting *RhNAC053*, *RhNAC092* and *RhSAG113*[34]. Our findings position AcMYB108 as a central positive regulator of IB through multiple lines of evidence: (i) its transcript abundance is markedly upregulated in IB tissues and correlates tightly with browning onset (Fig. 4A); (ii) transient overexpression in pineapple fruit significantly enhances IB incidence (Fig. 4B); (iii) its exclusive nuclear localization and C-terminal transcriptional activation activity supports a transcriptional regulator function (Fig. 4C-D). Notably, whereas AtMYB108 functions through targeting NAC-type transcription factors in *Arabidopsis*, our DAP-seq, Y1H and dual-luciferase assays uncovered AcWRKY31 and AcWRKY75 as direct downstream targets of AcMYB108 in pineapple. These WRKY transcription factors, in turn, activate the senescence-associated cysteine protease AcSAG12 (Fig. S1), thus establishing a regulatory cascade of MYB108→WRKY→SAG12.

Harvest maturity is known to influence IB susceptibility in pineapple[9]. Within the senescence framework established above, this observation can be explained through the developmental continuum linking fruit ripening to senescence[35]. Half-ripe fruits, being more advanced in this process and thus closer to senescence, may have a lower threshold for activating senescence-associated cascades such as AcMYB108→WRKY→SAG12. Conversely, color-break fruits remain at an earlier developmental stage and have not yet entered a state that facilitates rapid IB initiation. Thus, fruit maturity likely influences IB susceptibility by modulating the basal expression of senescence-associated genes, including the responsiveness of the AcMYB108-mediated cascade.

Gibberellins (GAs) are central phytohormones that coordinate diverse physiological processes from seed germination to fruit maturation while integrating environmental signals[36]. In pineapple, GAs have long been recognized as potent inducers of internal browning (IB), as both preharvest field applications and postharvest GA treatments exacerbate browning severity even under non-chilling conditions[20,21,37]. Previous studies have implicated GA in promoting browning through enhanced phenolic metabolism and increased polyphenol oxidase (PPO) activity[20], as well as through modulation of cell wall-degrading enzymes that may compromise tissue integrity[37]. However, these investigations have largely been descriptive, focusing on downstream biochemical changes rather than the upstream transcriptional regulatory events that orchestrate IB development.

Our findings demonstrate that GA promotes IB through two distinct routes that converge on the AcMYB108-mediated signaling cascade. At the transcriptional level, GA directly activates AcMYB108 expression, as evidenced by conserved GA-responsive GARE and P-box cis-elements identified in its promoter (Fig. S2A), and by approximately 5-fold transcriptional induction at 12 h post-GA treatment in

pineapple protoplasts (Fig. S2B). At the post-translational level, GA relieves the repressive constraint imposed by AcDELLA on AcWRKY75 activity. This regulatory module has been characterized in Arabidopsis, where DELLA proteins physically interact with WRKY transcription factors to suppress senescence-associated gene expression: DELLA protein RGL1 interacts with WRKY45 to inhibit WRKY-dependent SAG activation[38], while RGA binds WRKY6 to repress SAG13- and SGR-mediated senescence[39]. Our Y2H and BiFC assays confirmed a physical interaction between AcDELLA and AcWRKY75 (Fig. 8). In the presence of GA, 26S proteasome-mediated degradation of AcDELLA releases AcWRKY75, enabling its transcriptional activation of downstream senescence effectors, including AcSAG12. By simultaneously elevating the transcriptional activator AcMYB108 and removing its repressor AcDELLA, GA ensures robust activation of the senescence-associated program that drives IB in pineapple. This convergent regulation explains why GA exerts potent pro-browning effects even under non-chilling conditions, a phenomenon that the classical membrane-damage model fails to explain with.

Conclusions

In this study, we identified AcMYB108 as a key transcription factor in the senescence-associated regulation of postharvest internal browning in pineapple. We propose a working model wherein GA signaling and fruit maturity converge on the AcMYB108-mediated transcriptional cascade. Specifically, AcMYB108 directly activates AcWRKY31 and AcWRKY75, which subsequently induce the senescence-associated cysteine protease AcSAG12 to execute cellular degradation and browning manifestation. This AcMYB108-WRKY-SAG12 regulatory cascade establishes a direct molecular bridge between hormonal cues, developmental stage, and postharvest disorder. Our findings not only provide mechanistic insights into how GA treatment and fruit ripening influence IB susceptibility, but also identify potential targets for genetic or agronomic interventions to extend pineapple shelf life and reduce postharvest losses.

Abbreviations

IB – internal browning

GA –gibberellin

ABA – abscisic acid

DAP-seq – DNA affinity purification sequencing

Declarations

Authors' contributions

Han He, Chuanhe Liu, and Min Yang contributed to the conception and design of the study. Han He ,Chenping Zhou, Xiaming Wu and Yanzhao Sun performed the experiments analyzed the data. Chuanhe

Liu and Yuerong Wei supervised the project and revised the manuscript. All authors read and approved the final manuscript.

Funding

This research was supported by The Project of Collaborative Innovation Center of GDAAS (XTXM202203), Young Scientists Fund of the National Natural Science Foundation of China (32002018), Modern Agricultural Industry Technology System Innovation Team Construction Project of Guangdong Province (2026CXTD09).

Data availability

The data supporting the findings of this study are included in the article and Supplementary Information files. RNA-Seq data have been deposited in the NCBI database under accession numbers PRJNA1508263. The tissue-specific transcriptome data used in this study are available in the NCBI SRA database under accession number SRP156886.

Ethics approval and consent to participate

Not applicable.

Consent for publication

Not applicable.

Competing interests

The authors declare that they have no competing interests.

Acknowledgements

We are grateful to Dr. Xinxiang Peng, South China Agricultural University, Guangzhou, China, for generously providing the split-YFP constructs and for his helpful advice.

References

1. Li D, Jing M, Dai X et al. Current status of pineapple breeding, industrial development, and genetics in China[J].Euphytica, 2022, 218:85.
2. Luengwilai K, Beckles DM, Roessner U, et al. Identification of physiological changes and key metabolites coincident with postharvest internal browning of pineapple (Ananas comosus L.) fruit[J]. Postharvest Biol Technol. 2018;137:56–65.
3. Zhang Q, Liu Y, He C, et al. Postharvest exogenous application of abscisic acid reduces internal browning in pineapple[J]. J Agric Food Chem. 2015;63(22):5313–20.

4. Stewart RJ, Sawyer BJB, Bucheli CS, et al. Polyphenol oxidase is induced by chilling and wounding in pineapple[J]. Australian J Plant Physiol. 2001;28(3):181–91.
5. Zhou Y, Pan X, Qu H, et al. Low temperature alters plasma membrane lipid composition and ATPase activity of pineapple fruit during blackheart development[J]. J Bioenergetics. 2014;46(1):59–69.
6. Luengwilai K, Beckles DM, Siriphanich J. Postharvest internal browning of pineapple fruit originates at the phloem[J]. J Plant Physiol. 2016;202:121–33.
7. Zhang Q, Rao X, Zhang L et al. Mechanism of internal browning of pineapple: The role of gibberellins catabolism gene (AcGA2ox) and GAs[J].Scientific Reports, 2016, 6(1):33344.
8. Crouch EM, Jooste M, Majoni TJ, et al. Harvest maturity and storage duration influencing flesh browning in south african 'Cripps Pink' apples[J]. Acta Hort. 2015;1079:121–7.
9. Soares AG, Trugo LC, Botrel N, et al. Reduction of internal browning of pineapple fruit (Ananas comusus L.) by preharvest soil application of potassium[J]. Postharvest Biol Technol. 2005;35(2):201–7.
10. Mayer AM. Polyphenol oxidases in plants-recent progress[J]. Phytochemistry. 1986;26(1):11–20.
11. Leng P, Su S, Wei F et al. Correlation between browning, total phenolic content, polyphenol oxidase and several antioxidation enzymes during pistachio tissue culture[J]. Acta Hort, 2009(829):127–32.
12. Stewart RJ, Sawyer BJB, Robinson SP. Blackheart development following chilling in fruit of susceptible and resistant pineapple cultivars[J]. Aust J Exp Agric. 2002;42:195–9.
13. Hong K, Zhang L, Zhan R, Huang B, Song K, Jia Z. Identification and characterization of phospholipase D genes putatively involved in internal browning of pineapple during postharvest storage. Front Plant Sci. 2017;8:913.
14. Raimbault AK, Marie-Alphonsine PA, Horry JP, et al. Polyphenol oxidase and peroxidase expression in four pineapple varieties (Ananas comosus L.) after a chilling injury[J]. J Agric Food Chem. 2011;59(1):342–8.
15. Pusittigul I, Kondo S, Siriphanich J. Internal browning of pineapple (Ananas comosus L.) fruit and endogenous concentrations of abscisic acid and gibberellins during low temperature storage[J]. Sci Hort. 2012;146:45–51.
16. Bartlett A, O'Malley RC, Huang SSC, et al. Mapping genome-wide transcription-factor binding sites using DAP-seq[J]. Nat Protoc. 2017;12(8):1659–72.
17. Priyadarshani SVGN, Hu B, Li W et al. Simple protoplast isolation system for gene expression and protein interaction studies in pineapple (Ananas comosus L.)[J].Plant Methods, 2018, 14(1):1–12.
18. Yoo SD, Cho YH, Sheen J. Arabidopsis mesophyll protoplasts: a versatile cell system for transient gene expression analysis[J]. Nat Protoc. 2007;2(7):1565–72.
19. Niu FF, Cui X, Zhao PY, et al. WRKY42 transcription factor positively regulates leaf senescence through modulating SA and ROS synthesis in Arabidopsis thaliana[J]. Plant J. 2020;104(1):171–84.
20. Zhou YC, Dahler JM, Underhill SJ, R et al. Enzymes associated with blackheart development in pineapple fruit[J].Food Chemistry, 2003, 80(4):565–72.

21. Cano-Reinoso DM, Tamalea RR, Wibowo C. Physicochemical characteristic and internal browning of pineapple as affected by calcium and gibberellic acid dipping application[J]. Adv Hortic Sci. 2022;36(3):175–84.
22. Deuchande T, Carvalho SMP, ,Giné-Bordonaba J, et al. Transcriptional and biochemical regulation of internal browning disorder in 'Rocha' pear as affected by O2 and CO2 concentrations[J]. Postharvest Biol Technol. 2017;132:15–22.
23. Noushina I, Khan NA, Antonio F, et al. Ethylene Role in Plant Growth, Development and Senescence: Interaction with Other Phytohormones[J]. Front Plant Sci. 2017;08:475.
24. Setha S, Kongsuwan A, Srilaong V. Reduced Internal Browning in Pineapple Fruit by 1-MCP Pretreatment and the Antioxidant. Response[J] Acta Horticulturae. 2013;1012:573–9.
25. Selvarajah S, Bauchot AD, John P. Internal browning in cold-stored pineapples is suppressed by a postharvest application of 1-methylcyclopropene[J]. Postharvest Biol Technol. 2001;23(2):167–70.
26. Martins LP, Silva SM, Mendonça R M N et al. Postharvest quality of ‘Smooth Cayenne’ pineapple treated with 1-methylcyclopropene and cold shock[C].VII International Postharvest Symposium, 2012, 1012:503–508.
27. Suo J, Li H, Ban Q, et al. Characteristics of chilling injury-induced lignification in kiwifruit with different sensitivities to low temperatures[J]. Postharvest Biol Technol. 2018;135:8–18.
28. Woolf AB, Requejo-Tapia C, Cox KA, et al. 1-MCP reduces physiological storage disorders of 'Hass' avocados[J]. Postharvest Biol Technol. 2005;35(1):43–60.
29. Deell JR, Lum GB, Ehsani-Moghaddam B. Effects of multiple 1-methylcyclopropene treatments on apple fruit quality and disorders in controlled atmosphere storage[J]. Postharvest Biol Technol. 2016;111:93–8.
30. Cheng Y, Liu L, Feng Y et al. Effects of 1-MCP on fruit quality and core browning in 'Yali' pear during cold storage[J].Scientia Horticulturae, 2019, 243:350–6.
31. Huang S, Li T, Jiang G et al. 1-Methylcyclopropene reduces chilling injury of harvested okra (Hibiscus esculentus L.) pods[J].Scientia Horticulturae, 2012, 141:42–6.
32. Cao J, Liu HR, Tan SY et al. Transcription factors-regulated leaf senescence: current knowledge, challenges and approaches[J]. Int J Mol Sci 2023,24(11):9245.
33. Chou ML, Liao WY, Wei WC, et al. The direct involvement of dark-induced Tic55 protein in chlorophyll catabolism and its indirect role in the MYB108-NAC signaling pathway during leaf senescence in Arabidopsis thaliana[J]. Int J Mol Sci. 2018;19(7):1854.
34. Zhang S, Zhao Q, Zeng D, et al. RhMYB108, an R2R3-MYB transcription factor, is involved in ethylene- and JA-induced petal senescence in rose plants[J]. Hortic Res. 2019;6:131.
35. Gan S, Amasino. Making sense of senescence[J]. Plant Physiol. 1997;113:313–9.
36. Colebrook EH, Thomas SG, Phillips AL, et al. The role of gibberellin signalling in plant responses to abiotic stress[J]. J Exp Biol. 2014;217(1):67–75.

37. Li Q, Wang G, Zhang L, et al. AcbHLH144 transcription factor negatively regulates phenolic biosynthesis to modulate pineapple internal browning[J]. Hortic Res. 2023;10(10):uhad185.
38. Chen L, Xiang S, Chen Y, et al. Arabidopsis WRKY45 interacts with the DELLA protein RGL1 to positively regulate age-triggered leaf senescence[J]. Mol Plant. 2017;10(9):1174–89.
39. Zhang LP, Chen LG, Yu DQ, et al. Transcription factor WRKY75 interacts with DELLA proteins to affect flowering[J]. Plant Physiol. 2018;176(1):790–803.

Figures

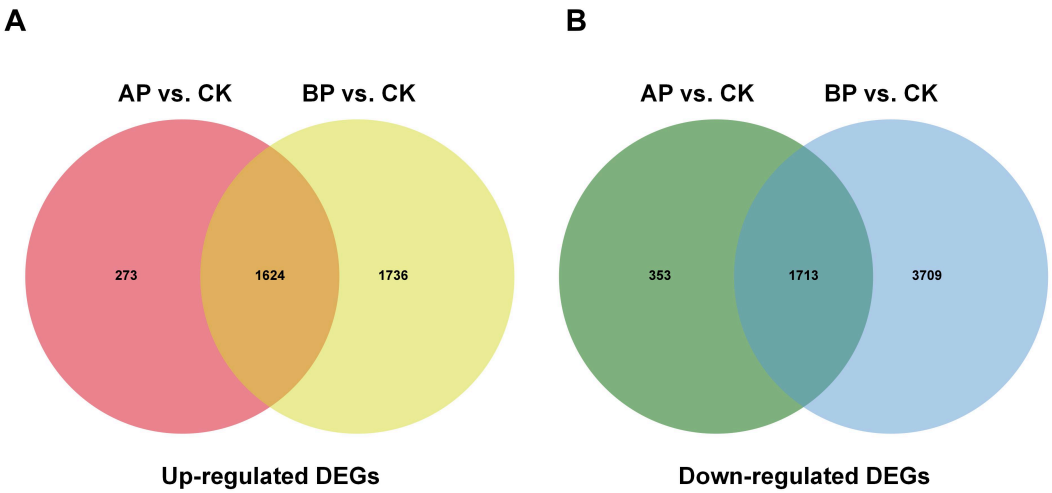


Figure 1

Figure 1

Venn diagrams showing the overlap of differentially expressed genes (DEGs) among different pulp tissue types at the onset of internal browning. (A) Up-regulated DEGs. (B) Down-regulated DEGs. DEGs were identified by pairwise comparisons of browning pulp (BP) and adjacent non-browning pulp (AP) against control pulp (CK), using thresholds of $|\log_2 FC| \geq 1$ and FDR ≤ 0.01.

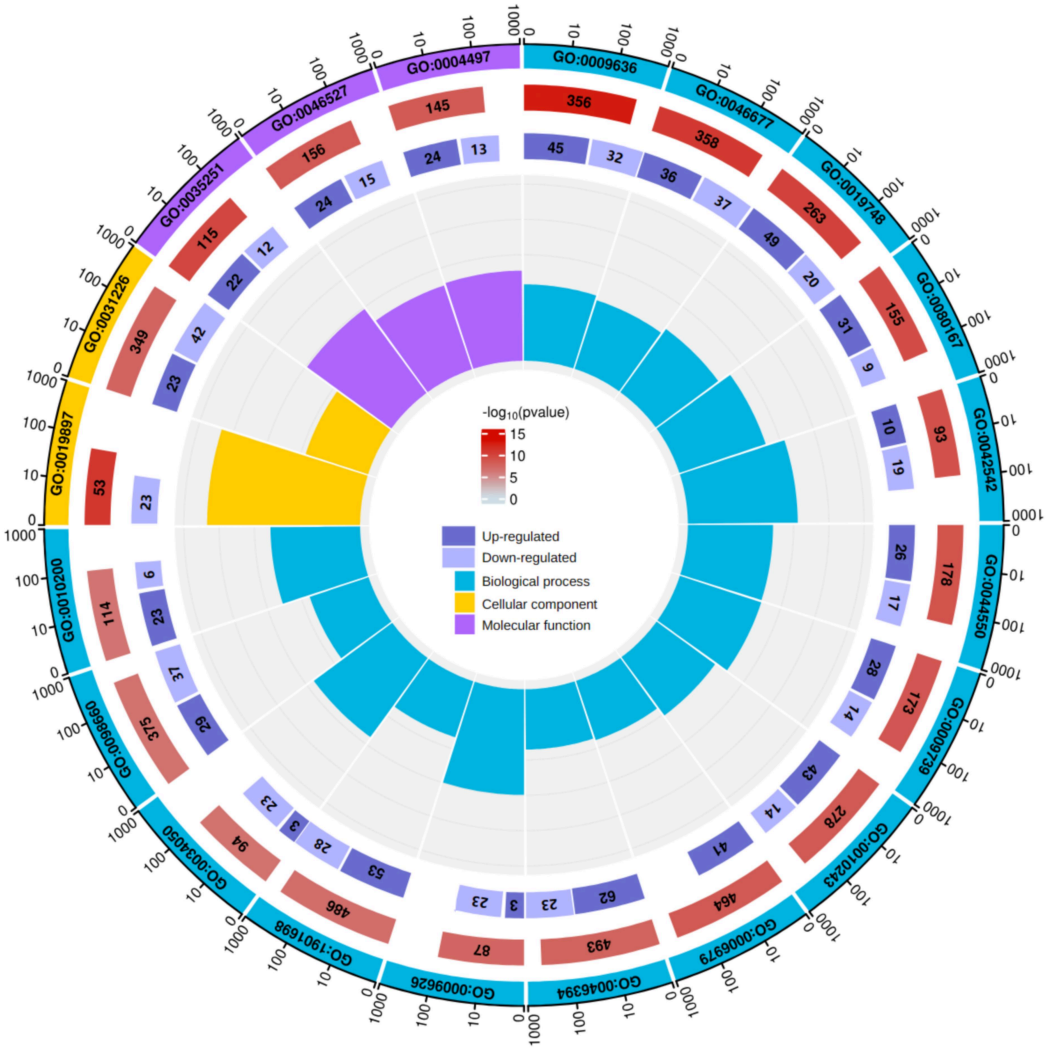


Figure 2

Figure 2

Circular visualization of Gene Ontology (GO) enrichment analysis of DEGs associated with internal browning. Enriched GO terms are categorized into three main classes: biological process (blue), cellular component (yellow) and molecular function (purple). From the outermost to the innermost ring, the plot displays: (1) the identifier numbers of the top enriched GO terms; (2) the number of DEGs per term (bar height) and the corresponding enrichment significance (color gradient based on -$\log_{10}$(P-value)); (3) the proportional distribution of up-regulated (dark blue) and down-regulated (light blue) DEGs within each

GO term; (4) the rich factor, calculated as the ratio of the number of DEGs annotated to a given GO term to the total number of background genes annotated to that term.

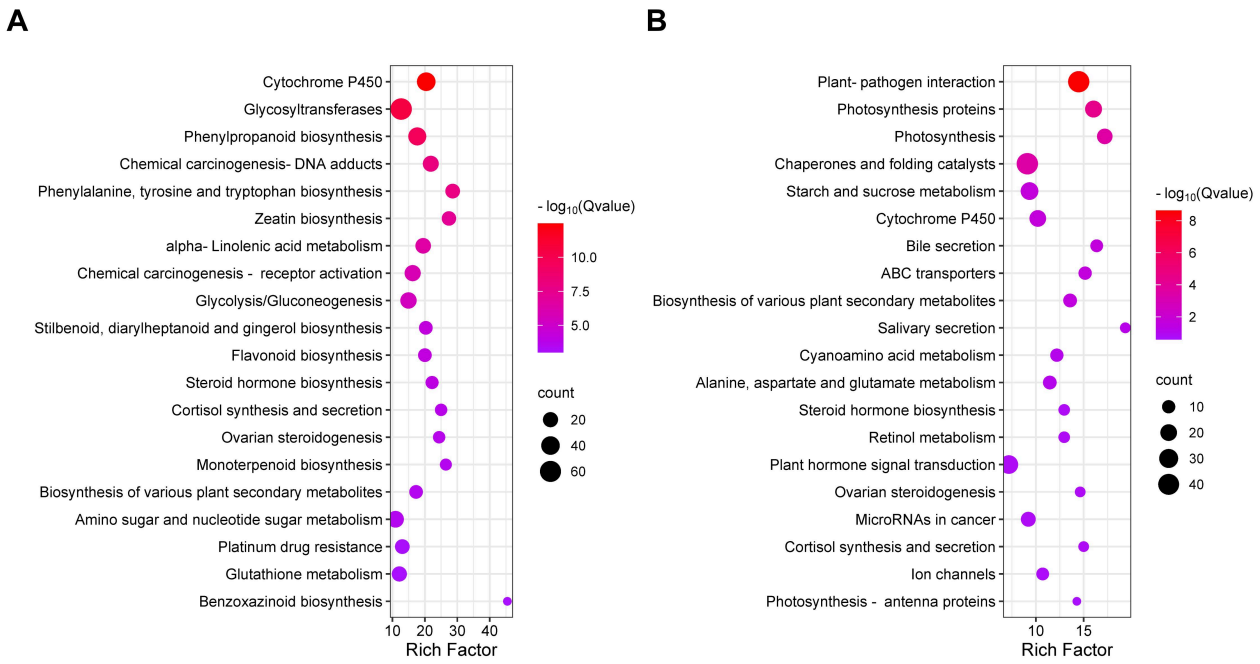


Figure 3

Figure 3

KEGG pathway enrichment bubble plots of DEGs associated with internal browning. (A) Up-regulated pathways. (B) Down-regulated pathways. The x-axis represents the rich factor, bubble size indicates the number of enriched DEGs, and color denotes Q-value significance (red: low Q-value; blue: high Q-value).

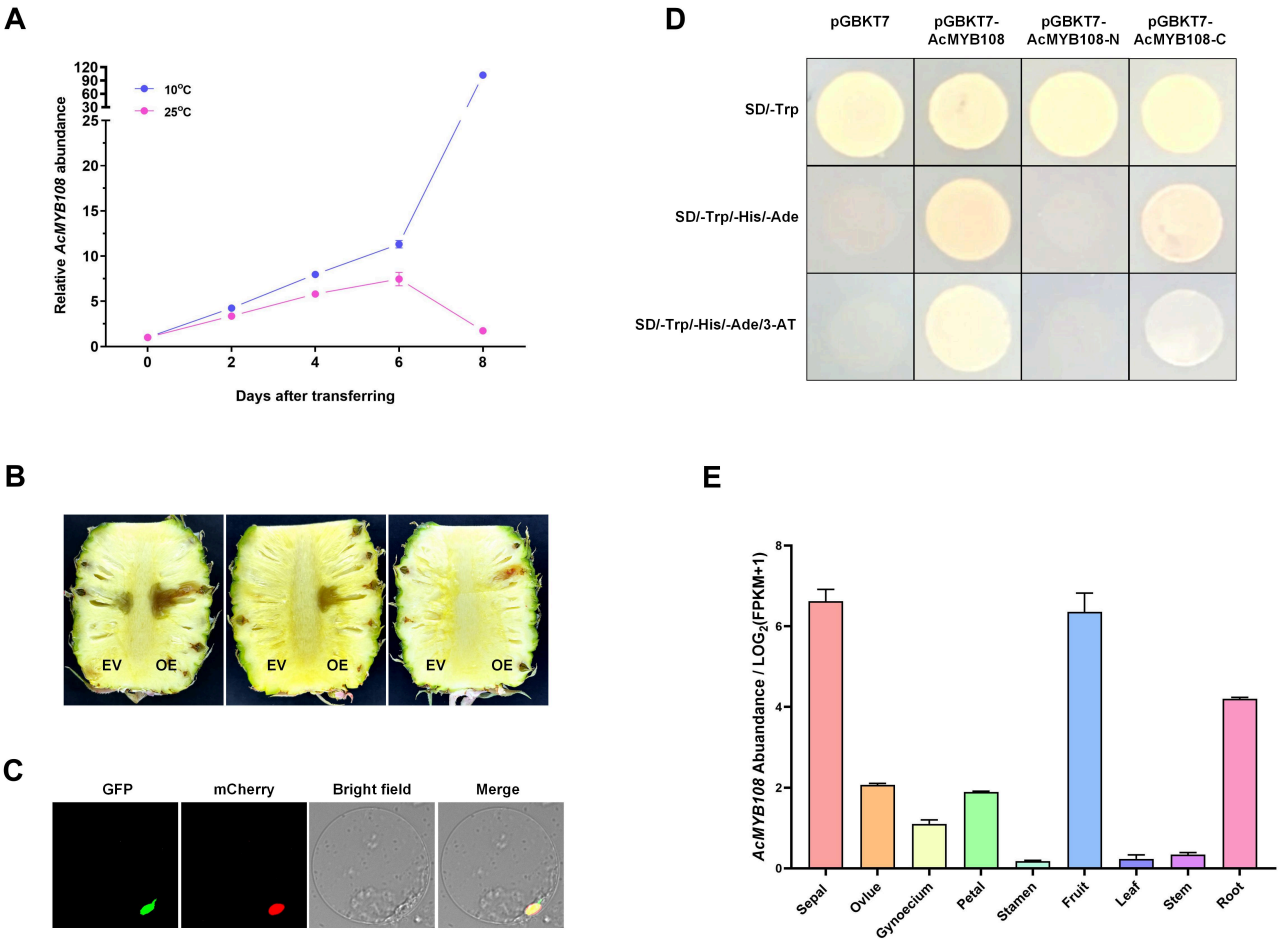


Figure 4

Figure 4

Functional characterization of AcMYB108 in pineapple. (A) Temperature-dependent expression profiles of AcMYB108. Relative transcript levels in postharvest pineapple fruits stored at 10°C(blue) and 25°C (purple) were determined by qRT-PCR. Data are presented as means ±SD (n = 3 biological replicates). (B) Transient overexpression of AcMYB108 in pineapple fruit pulp. Representative images of infiltration zones at 4 days post-agroinfiltration (dpi). Left: empty vector (EV) control; right: AcMYB108 overexpressing construct (OE). (C) Subcellular localization of AcMYB108. Pineapple protoplasts co-

expressing AcMYB108-GFP and the nuclear marker NLS-mCherry. The merged image shows overlapping GFP and mCherry signals, indicating nuclear localization of AcMYB108. (D) Transcriptional activation assay of AcMYB108 deletion variants in yeast. AcMYB108-N (C-terminal truncation) and AcMYB108-C (N-terminal truncation) were fused to the GAL4 DNA-binding domain in pGBKT7. Empty pGBKT7 vector served as a negative control. Growth on SD/-Trp/-His/-Ade selective medium indicates transcriptional activation activity. (E) Tissue-specific expression of AcMYB108. Relative transcript abundance of*AcMYB108* in nine different pineapple tissues.

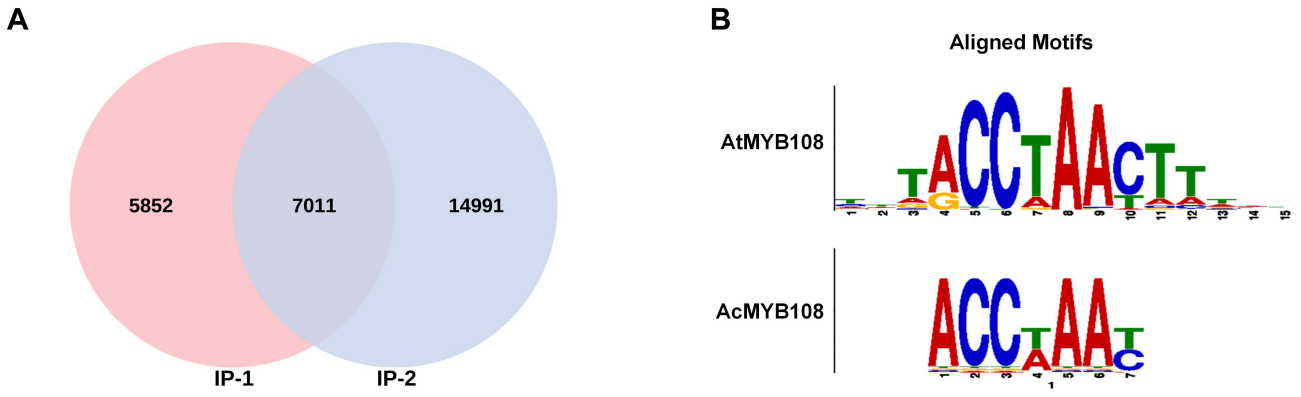


Figure 5

Figure 5

Genome-wide identification of AcMYB108 binding sites by DAP-Seq. (A) Venn diagram showing overlap of AcMYB108-associated peaks between two biological replicates (FDR < 0.01, fold enrichment ≥ 2).

(B) DNA-binding motif comparison between AcMYB108 and Arabidopsis AtMYB108 (MA2026.1, JASPAR).

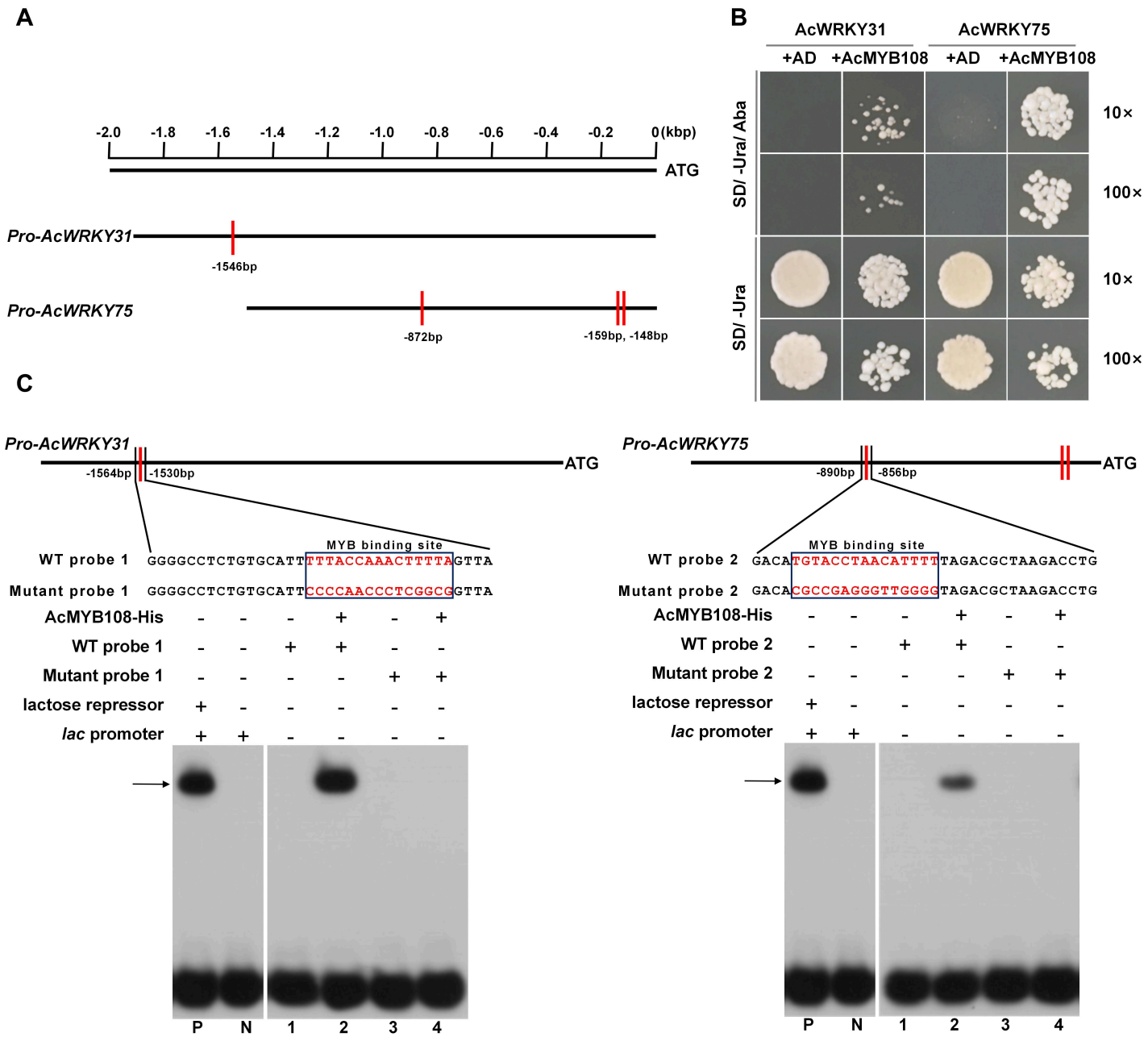


Figure 6

Figure 6

AcMYB108 directly binds to the promoters of AcWRKY31 and AcWRKY75. (A) Promoter schematics of AcWRKY31 and AcWRKY75. Red bars indicate putative MYB binding sites, and numbers denote positions relative to ATG (+1). (B) Y1H assays showing AcMYB108-promoter interactions. Growth on SD/-Leu + 200 ng/mL AbA indicates positive interaction. Empty pGADT7 was used as negative control. (C) EMSA validating direct binding. Biotin-labeled WT probes and mutant probes (with MYB binding site in red) were incubated with recombinant AcMYB108, arrows indicate shifted complexes. Full-length blots are presented in Supplementary Figure S3.

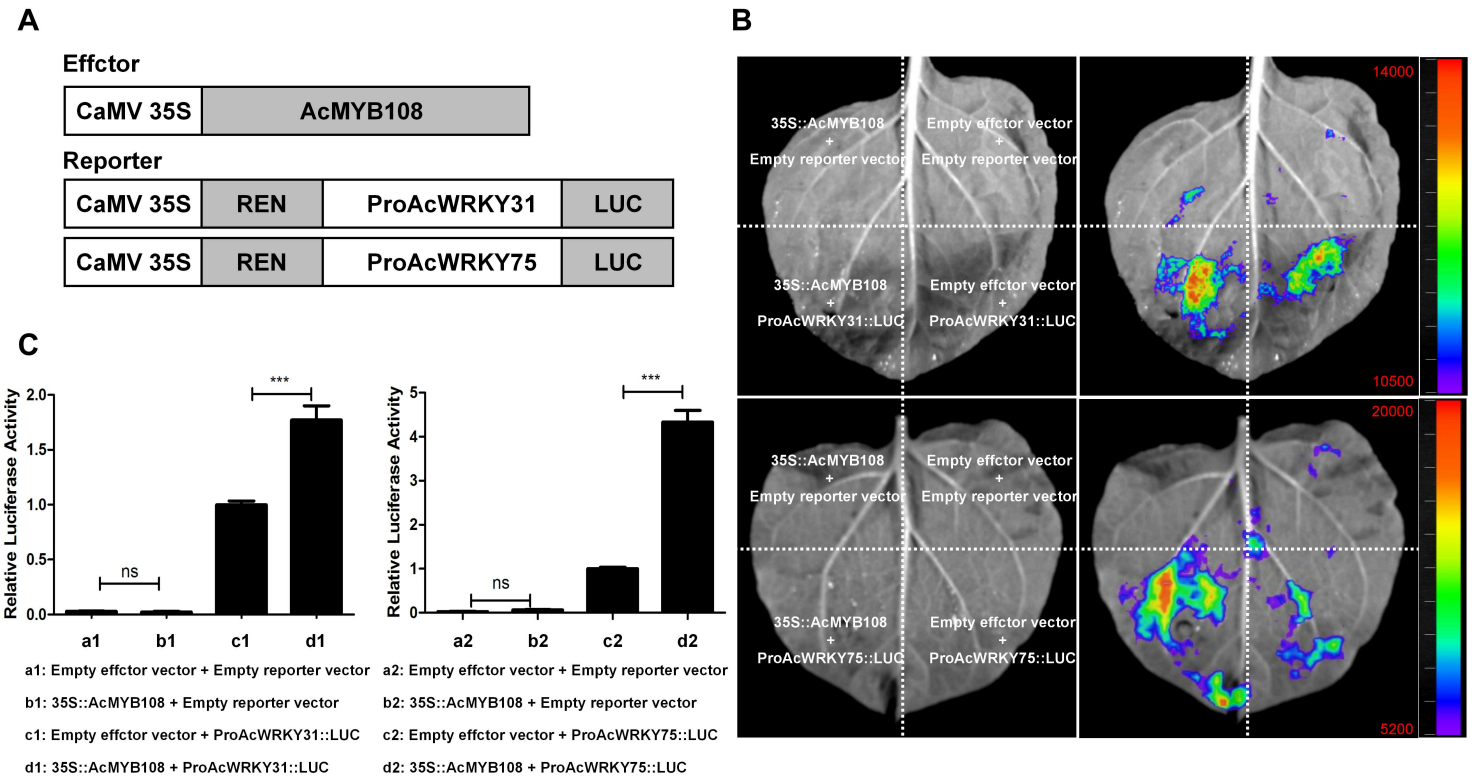


Figure 7

Figure 7

AcMYB108 trans-activates the AcWRKY31 and AcWRKY75 promoters in a dual-LUC assay. (A) Schematic of effector and reporter constructs. (B) Chemiluminescence images of LUC activity in *Nicotiana benthamiana* leaves at 48 hours post-agroinfiltration. (C) Normalized LUC/REN ratios (means±SD, n = 5). Significance was determined by student's t-test (*P < 0.05, **P < 0.01) relative to empty vector controls.

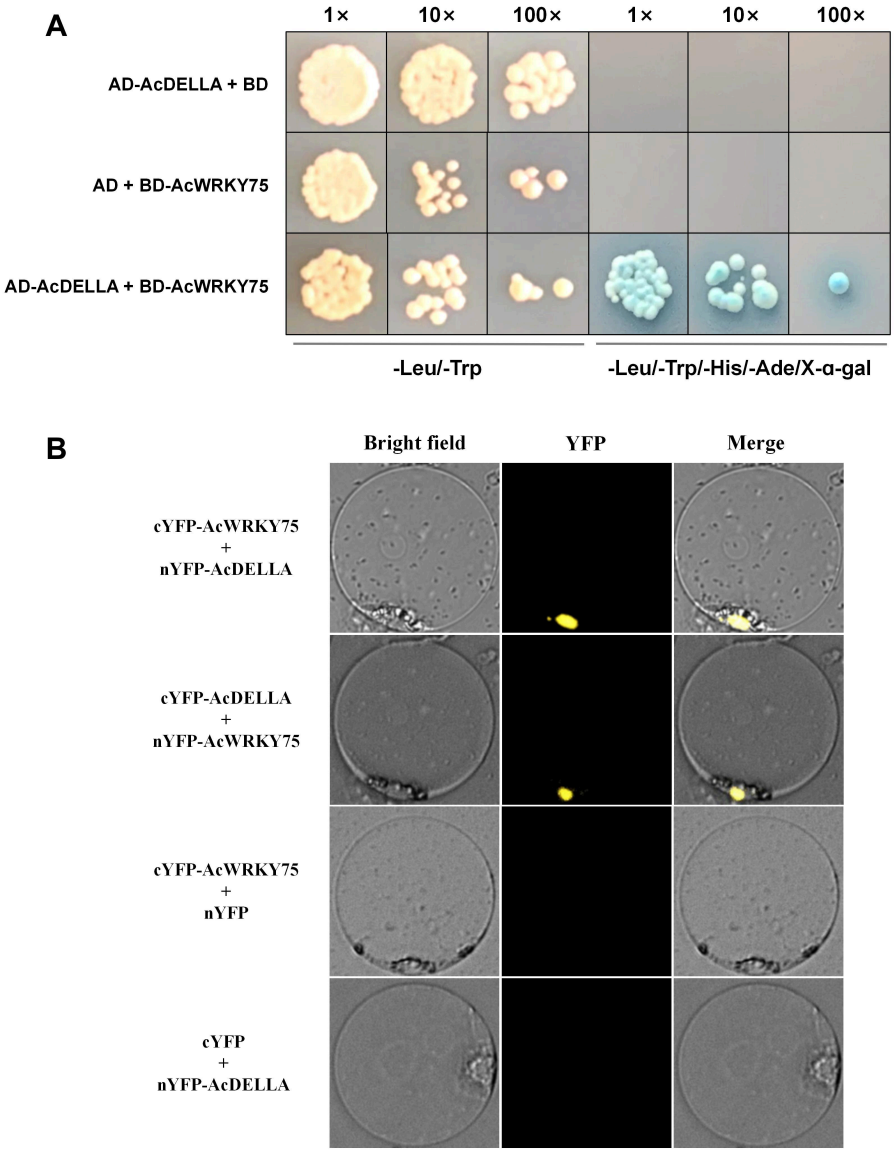


Figure 8

Figure 8

AcWRKY75 interacts with AcDELLA in yeast and plant cells. (A) Y2H assay. BD-AcWRKY75 + AD-AcDELLA were co-transformed into Y2HGold. Growth and blue color on SD/-Leu/-Trp/-His/-Ade + X-α-Gal indicate interaction. BD + AD-AcDELLA and BD-AcWRKY75 + AD served as negative controls. (B) BiFC assay in pineapple protoplasts. YFP fluorescence was reconstituted by cYFP-AcWRKY75 + nYFP-AcDELLA and cYFP-AcDELLA + nYFP-AcWRKY75, but not by controls lacking either fusion partner.

Supplementary Files

This is a list of supplementary files associated with this preprint. Click to download.

- FigureS1.jpg
- FigureS2.jpg
- FigureS3.jpg
- TableS1.xlsx